PCCP

Accepted Manuscript

ROYAL SOCIETY OF CHEMISTRY

www.rsc.org/pccp

Cite this: DOI: 10.1039/c0xx00000x

www.rsc.org/xxxxxx

ARTICLE TYPE

Plasmonic circular dichroism in side-by-side oligomers of gold nanorods: influence of chiral molecule location and interparticle distance

Shuai Hou,[a,b] Hui Zhang,[a,b] Jiao Yan,[a,b] Yinglu Ji,[a] Tao Wen,[a,b] Wenqi Liu,[a,b] Zhijian Hu,*[a] and Xiaochun Wu*[a]

Received (in XXX, XXX) Xth XXXXXXXXX 20XX, Accepted Xth XXXXXXXXX 20XX
DOI: 10.1039/b000000x

Chiral metal nanostructures, which exhibit plasmonic circular dichroism (PCD), have great potential for the development of chiral sensors and devices. Previously, we developed a method for fabricating chiral gold-nanorod oligomers: the nanorods are linked by achiral molecules, while chiral molecules (*e.g.* L- or D-cysteine) on the Au surface exert a directional twisting force on the oligomers and thereby generate a PCD signal. In this paper, we investigate how the location of chiral molecules and the interparticle distance affect PCD of the oligomers. Cysteine at the ends of the nanorods and those on the side were found to induce PCD with opposite signs. When we increased the interparticle distance, the PCD signal was weakened; in particular, cysteine at the ends lost the twisting effect. Besides introducing the twisting force at the Au surface, chiral molecules in the hydrophobic surfactant bilayer and those adsorbed outside the surfactants can also twist the oligomers and generate PCD signals. These findings not only provide guidelines to the manipulation of PCD signals, but also serve as a more elaborate platform for studying the nanoscale interactions between nanoparticles.

1. Introduction

Metal nanostructures, through the excitation of surface plasmon resonance (SPR), interact strongly with light. If the metal nanostructures are chiral, *i.e.*, their mirror images cannot be imposed to themselves, their interactions with left- and right-circularly polarized lights are different; the differential optical extinction is termed circular dichroism (CD).[1] Because of its relation with plasmon resonance, CD in metal nanostructures is usually referred to as plasmonic CD (PCD).[2,3] PCD is intense and often lies in the visible or near-infrared spectral range, which makes it particularly promising for applications in optical devices and biosensors.[4–7] Considering the high cost of lithographic methods for building chiral nanostructures, a bottom-up approach, in which metal nanoparticles synthesized via wet chemistry are arranged into chiral configurations, offers an alternative strategy.[8–18] Among commonly used metal nanoparticles, gold nanorods (GNRs) receive more and more attention.[11–18] Thanks to the geometric anisotropy of GNRs, GNR-based chiral structures are much easier to fabricate than their spherical counterpart. Only two nanorods are required for a chiral configuration;[15–19] for example, chiral dimers with the out-of-plane "X" and "L" shapes have been realized based on DNA origami templates.[16–18] Moreover, the longitudinal SPR of GNRs is sensitive to the aspect ratio of the rods, which facilitates fine-tuning in the spectral ranges of the PCD bands.[13,14,20] Although substantial progress has been made in the fabrication of chiral assemblies of metal nanoparticles, more efforts are needed for a better control over the PCD signal, which has to rely on a comprehensive understanding of its influencing factors.

Our previous study has demonstrated an easy yet powerful way to fabricate chiral GNR oligomers.[14] Unlike most of the previously reported systems, where chiral molecules were used to link the GNRs,[8,15,20] chiral molecules and linkers are separated in our method: we use the achiral molecule citrate to link the GNRs in a side-by-side (SS) fashion and employ chiral molecules such as cysteine (CYS) to twist the oligomers. The linking ability of citrate originates from the electrostatic interaction between the positively charged GNRs and the negatively charged citrate ions. CYS molecules adsorbed on the Au surface, although not directly linking the GNRs, are able to exert a directional twisting force on the oligomers and thus producing PCD signals. The sign and the magnitude of PCD signals are determined by the twist angle. For example, twist angles with equal magnitude but opposite signs result in PCD signals with mirror symmetry, and a larger twist angle indicates a stronger PCD signal (note that this is not true when the twist angle is large, *e.g.*, larger than 45°, which is not the case here because the twist angle in the SS oligomers is usually very small).[14,15] Although the exact nature of the twisting force is still unknown, it may be manipulated in several ways in order to control the PCD signal. In this paper, we investigate the influence of two crucial factors, namely, the location of chiral molecules and the distance between the GNRs (Scheme 1). The flexibility of our fabrication method allows us to study the two factors separately: the location of CYS on the nanorod surface (at

the ends or on the side) was controlled by changing the concentration of CYS and by other surface modifications as will be explained later; the interparticle distance was controlled by using linkers of different sizes. Based on these designs, we will show that the twisting of the oligomers is extremely sensitive to the location of CYS on the nanorod surface and the spacing between the rods. These results highlight the complexity involved in the nanoscale interactions between the nanorods.

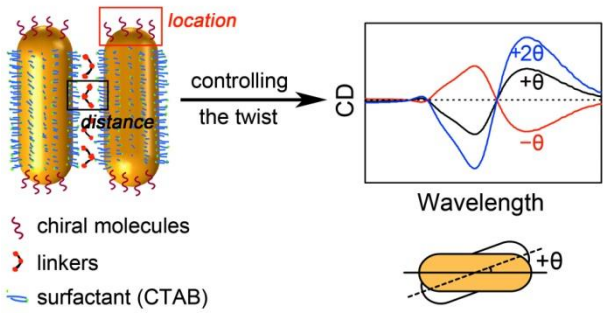

Scheme 1 Manipulation of PCD signals by controlling the twisting of gold-nanorod oligomers, which is sensitive to the chiral molecule location and the interparticle distance.

2. Methods

2.1 Chemicals

Chloroauric acid ($HAuCl_4 \cdot 3H_2O$), silver nitrate ($AgNO_3$), sodium hydroxide (NaOH), and hydrochloric acid (HCl) were purchased from Beijing Chemical Reagent Company. Sodium borohydride ($NaBH_4$), cetyltrimethylammonium bromide (CTAB), L-ascobic acid (AA), trisodium citrate, L-cysteine (L-CYS), D-cysteine (D-CYS), L-glutathione (L-GSH), N-acetyl-L-cysteine (L-NAC), and bovine serum albumin (BSA) were purchased from Sigma Aldrich. 4-mercaptopyridine (4MP), (R)-(+)-1,1'-binaphthyl-2,2'-diamine (BNA), and poly(amido amine) dendrimers (PAMAM, generation 3.5) were purchased from Acros Organics. HS-C_{11}-$(EG)_6$-OMe (PEG-OMe) and HS-C_{11}-$(EG)_6$-OCH_2-COOH (PEG-COOH) were purchased from ProChimia.

2.2 Preparation of the GNRs and surface modification

Three kinds of GNRs with different surface modifications were used: the normal CTAB-coated GNRs, GNRs whose ends are blocked by PEG-OMe, and GNRs with a thin silver coating.

The CTAB-coated GNRs were synthesized using a modified seed-mediated method.[14] After two rounds of washing (9200 rpm, 10 min), the precipitates were resuspended in water containing 0.5 mM CTAB, and the concentration of the GNRs was adjusted to 90 pM according to the molar extinction coefficient of GNRs at 400 nm.[14]

For end-blocking of the GNRs, a calculated volume of 0.1 mM PEG-OMe solution was added into the above GNR solution to obtain a PEG-OMe concentration of 1 μM. The resulting solution was kept at 30 ºC for 30 min before further use.

For silver coating on the GNRs, 4 mL of the GNR solution was mixed with 4 mL of 0.1M CTAB solution and 4 mL of water, followed by the sequential addition of $AgNO_3$ (10 mM, 48 μL), NaOH (0.2 M, 110 μL), and AA (0.1M, 110 μL). The solution was kept at 30 ºC for more than 3 h. After washing twice (9000 rpm, 10 min), the precipitates was resuspended in 4 mL of water with 0.5 mM CTAB.

2.3 Preparation of the SS oligomers

The trisodium citrate solution (15 μL, 10 mM) or the PAMAM dendrimer solution (15 μL, 0.45 mM) was added into 1 mM of the GNR solution to trigger the formation of oligomers. The reaction completes within 30 min. This method applied to all three kinds of GNRs.

Different kinds of chiral molecules were added to twist the oligomers. For L-CYS, 10 μL of L-CYS solution with different concentrations were added before adding the linkers. For BNA, 10 μL of 1 mM BNA in ethanol was added prior to the addition of linkers. For BSA, 100 μL of BSA solution (5% in 0.1 M phosphate buffer, pH 7.4) was added after the formation of oligomers.

2.4 PEG-COOH-linked SS assembly

PEG-COOH (15 μL, 1 mM) was added into 1 mL of GNR solution ([CTAB] ≈ 10 μM) for ligand exchange. The same amount of L-CYS was then added and incubated for 30 min. When the pH value was adjusted to 3 by adding HCl, SS assembly occurred. If the pH value was adjusted back to 7, the SS oligomers were dissociated.

2.5 Instrumentation

CD measurements were conducted on a JASCO J-810 CD spectrometer, the bandwidth was set to be 5 nm. All CD spectra of the SS oligomers were acquired 30 min after the formation of oligomers. The extinction spectra were obtained from a Cary 50 UV-vis-NIR spectrophotometer. Raman spectra were obtained in the solution phase using a Renishaw InVia Raman microscope. TEM images were taken from a Tecnai G^2 20 S-TWIN TEM with an accelerating voltage of 200 kV.

2.6 Finite element method (FEM) calculations

FEM calculations were performed using the RF module of COMSOL Multiphysics. A GNR was modeled as a cylinder with two hemispherical caps. Its dimension was set to be 64 nm by 22 nm according to the TEM measurement. The refractive index of the surrounding medium was set to be 1.33, and the dielectric function of gold was adopted from the experimental data by Johnson and Christy.[21] In the calculation of electric field profiles around an SS tetramer, the interparticle gap was set to be 4 nm; the incident light was linearly polarized, with polarization parallel to either the longitudinal or transverse axis of the nanorod. To explore the effect of interparticle distance, we calculated the PCD intensity of a dimer with 1° twist angle, and the interparticle gap was varied between 4 nm and 20 nm; the incident light was circularly polarized. CD was calculated as the difference between the extinction of left- and right-circularly polarized light and was averaged over three orthogonal directions of light incidence.

3. Results and discussion

3.1 Influence of the chiral molecule location

Since chiral molecules are the origin of PCD in the SS oligomers, one would expect a monotonic increase of the signal with increasing concentration of L-CYS. However, our results show

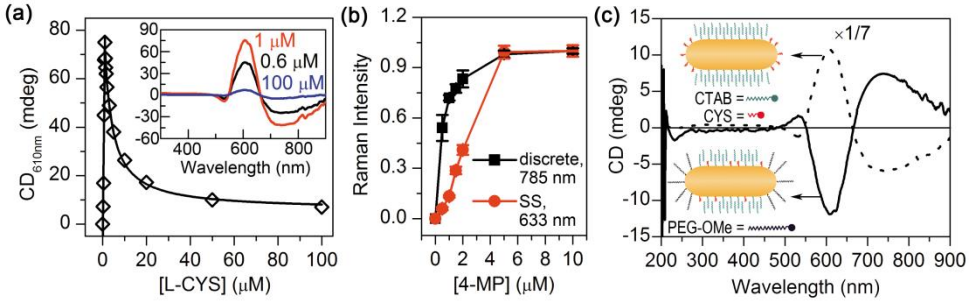

Fig. 1 Influence of the L-CYS location on the PCD of citrate-linked oligomers. (a) PCD intensity at 610 nm as a function of L-CYS concentration. Inset: CD spectra of citrate-linked oligomers with 0.6 μM, 1 μM, and 10 μM L-CYS. (b) Location change of L-CYS as revealed by SERS intensity of 4-MP with increasing concentrations. Black squares: discrete GNRs excited by a 785 nm laser; red circles: SS oligomers excited by a 633 nm laser. (c) CD spectra of the oligomers with L-CYS preferentially on the side of GNRs (solid line, [PEG-OMe] = 1 μM and [L-CYS] = 10 μM) compared with L-CYS specifically at the ends (dotted line, [L-CYS] = 1 μM).

otherwise. As shown in Fig. 1a, the PCD signal of the citrate-linked SS oligomers has a maximum value when 1 μM L-CYS is used. As the concentration of L-CYS further increases, the PCD signal reduces from 75 mdeg to 7 mdeg at 610 nm. This trend is not limited to L-CYS, but was also found when N-acetyl-L-cysteine or L-glutathione were used to modify the GNRs (Fig. S1, ESI†). Interestingly, the concentration corresponding to the maximum PCD was around 1 μM for all three molecules. Considering the difference in molecular structure of the three molecules, the trend reversal of PCD signal is most likely related to the nanorods themselves (*e.g.*, their surface chemistry) rather than the nature of chiral molecules. There are abundant evidences in the literature that thiols at low concentration are preferentially bound to the ends of GNRs, and they expand to the side at high concentrations.[22,23] This surface chemical anisotropy is due to less ordered CTAB bilayer at the ends and a much denser one on the side.[23] We make two hypotheses to explain why there exists a maximum PCD signal with 1 μM L-CYS. First, the threshold concentration for CYS to bind to the side of GNRs is around 1 μM. Second, CYS at the ends and those on the side tend to twist the oligomers to opposite directions, so that the net PCD signal is reduced when CYS are on both the ends and the side of the GNRs.

To prove the first hypothesis, we used surface enhanced Raman spectroscopy (SERS) to determine the change of CYS distribution on the rod surface with increasing CYS concentration. The Raman signal of CYS is too weak for quantitative analysis; therefore, 4-mercaptopyridine (4-MP) was used instead as the Raman reporter. According to electromagnetic field calculations (Fig. S2, ESI†), the electric field is much stronger at the ends than the field at the side for the discrete GNRs when excited by a 785 nm laser; but for SS oligomers excited by a 633 nm laser, the intensity difference between electromagnetic field at the ends and that on the side is small. Since the SERS signals are mainly contributed from 4-MP molecules that are in strong electric fields, the SERS signal of 4-MP on discrete GNRs reflects the amount of 4-MP adsorbed at the ends of the GNRs, while the SERS signal of 4-MP on SS oligomers should roughly reflect the amount of 4-MP on the whole surface of the GNRs. According to Fig. 1b (the corresponding SERS spectra are presented in Fig. S3, ESI†), SERS signal from the ends of GNRs (black squares) is almost saturated when the concentration of 4-MP is higher than 1 μM, but that from the whole surface of GNRs (red circles) continues to grow, indicating that 4-MP (and L-CYS similarly) mainly adsorbs on the side after 1 μM.

To test the second hypothesis that L-CYS at the ends and those on the side twist the oligomers to opposite directions, we modified the GNRs with L-CYS specifically on the side by blocking both ends with the achiral HS-C_{11}-$(EG)_6$-OMe (termed PEG-OMe). The blocking effect of PEG-OMe was confirmed and visualized by growing silver on the PEG-OMe modified GNRs (Fig. S4, ESI†). Without PEG-OMe, both the ends and the side of the GNRs were coated with Ag. When 1 μM PEG-OMe was used, the growth of Ag on the ends of GNRs was completely blocked, and the Ag coating was only on the side of the GNRs. As the concentration of PEG-OMe was further increased to 10 μM, no Ag was coated on the rods, suggesting the whole surface of the rod was blocked. Accordingly, 1 μM PEG-OMe was used to block the ends, and the subsequently added L-CYS (10 μM) was expected to preferentially bind to the side of the GNRs. After formation of the SS oligomers by adding citrate, a PCD signal with an opposite sign was observed (Fig. 2c solid line). Thus, the trend reversal of PCD signal, which occurs when L-CYS concentration is 1μM, is a reflection of location shift of the chiral molecules on the nanorods.

3.2 Influence of the interparticle distance

To obtain SS oligomers with enlarged interparticle distance, we used the anionic poly(amido amine) dendrimer (PAMAM, generation 3.5) as linkers, as shown in Fig. 2a. The gap size increased from 4.3 ± 1.4 nm between the citrate-linked GNRs to 5.9 ± 1.8 nm according to TEM measurments. The experimental conditions are identical to the citrate case except for the size of linkers; therefore, 1 μM is still the threshold concentration associated with location shift of L-CYS. Fig. 2a shows the PCD signals (at 628 nm) plotted against the concentration of L-CYS. We were surprised to note the following results. First, when [L-CYS] < 1 μM, *i.e.*, L-CYS was at the ends of the GNRs, only a very faint PCD signal was observed (ca. 2 mdeg). Then, when [L-CYS] > 1 μM, *i.e.*, CYS molecules expand to the side of GNRs, the sign of PCD signal flipped opposite to the citrate-linked oligomers. The magnitude of PCD signal induced by L-CYS on the side of GNRs was also weakened: when the concentration of L-CYS was 100 μM, L-CYS on the side contributed –37 mdeg in the dendrimer-linked oligomers, which is only a half of that in the

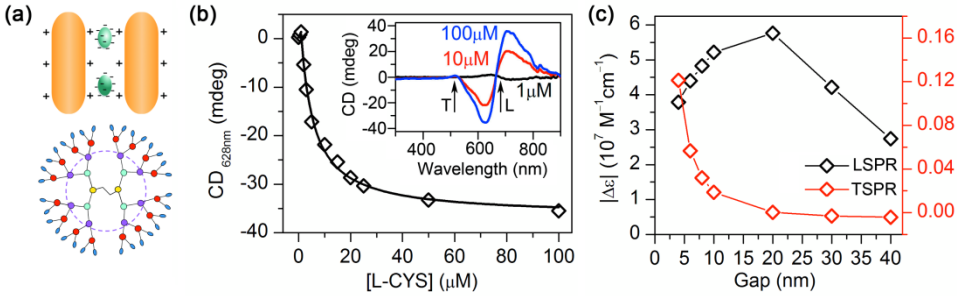

Fig. 2 Dendrimer-linked SS oligomers: influence of the gap size. (a) Top: Illustration of a dendrimer-linked SS dimer highlighting the electrostatic driving force of the assembly. Bottom: Chemical structure of the PAMAM dendrimer (spheres: tertiary N, ellipsoids: -COOH, lines: -$(CH_2)_2$-CONH-$(CH_2)_2$-). (b) CD signal at 628 nm as a function of L-CYS concentration. Inset: CD spectra of the oligomers with 1 μM, 10 μM, and 100 μM L-CYS. (c) Calculated CD intensity of an SS dimer with a 1° twist angle and various gap sizes. The wavelength of LSPR and TSPR are represented in (b) by arrows with L and T, respectively. The CD intensity of the LSPR mode is taken as the average height of the positive peak and negative dip.

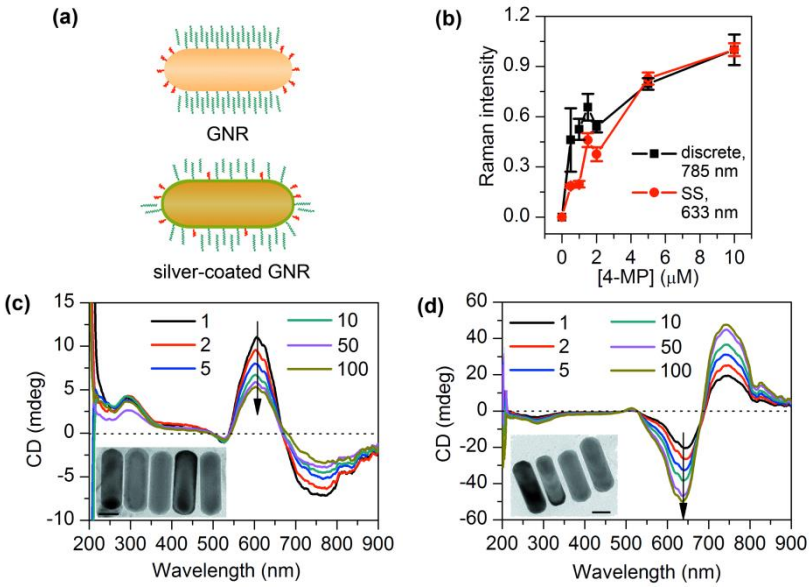

Fig. 3 PCD in SS oligomers of silver-coated GNRs: influence of surface chemistry. (a) A comparison between L-CYS distribution on normal and silver-coated GNRs modified with 1 μM L-CYS. (b) Distribution of thiols on the nanorod surface as revealed by the SERS intensity of 4-mercaptopyridine. (c) CD spectra of citrate-linked oligomers with L-CYS concentration ranging from 1 μM to 100 μM. (d) CD spectra of dendrimer-linked oligomers with L-CYS concentration ranging from 1 μM to 100 μM. Insets: TEM images of the oligomers (scale bar: 20 nm).

citrate-linked oligomers (−68 mdeg). Despite these differences, there is consistency in the two systems with different linkers, that is, L-CYS at the ends and those on the side tend to twist the oligomers to opposite directions. And this is exactly why the sign of PCD signal flipped when [L-CYS] > 1 μM.

There are two possible explanations for the reduction of PCD signal when the gap is larger. The first is simply that the twist angle becomes smaller. And the second is that the plasmon coupling between the nanorods becomes weaker, which might result in smaller PCD signals for oligomers with the same twist angle but larger interparticle distance. To test the influence of plasmon coupling, we calculated the PCD intensity for a chiral dimer with a 1° twist angle and various gap sizes. The results are shown in Fig. 2c. PCD signal of the longitudinal SPR (LSPR) mode, taken as the average height of the positive peak and the negative dip, slightly increases with the increase in interparticle distance when the gap size is smaller than 20 nm, which is consistent with previous calculations.[7] Therefore, the second explanation is rejected, and the weakened PCD signal observed for the LSPR mode is mainly due to smaller twist angles. Considering the small size of CYS, the acting region of the twisting force is limited. At enlarged interparticle distances, the decreased twisting force may lead to smaller twist angles and hence smaller PCD signals. Meanwhile, the PCD signal corresponding to the transverse SPR (TSPR) mode is drastically reduced, which is due to both reduced twist angle and weakened plasmon coupling (see calculation in Fig. 2c, red squares).

3.3 PCD in the SS oligomers of silver-coated GNRs

To further demonstrate the importance of the chiral molecule location and the interparticle distance, we altered the surface chemistry of GNRs by coating them with a thin silver shell. Gold and silver show different surface chemistry: the binding of CTAB bilayer to the side of silver-coated GNRs is weaker than that in the case of normal GNRs.[24] This means that thiols at low concentrations can also bind to the side of the rods after silver coating (Fig. 3a). To confirm the change in surface chemistry, again we resort to SERS to determine the molecule distribution

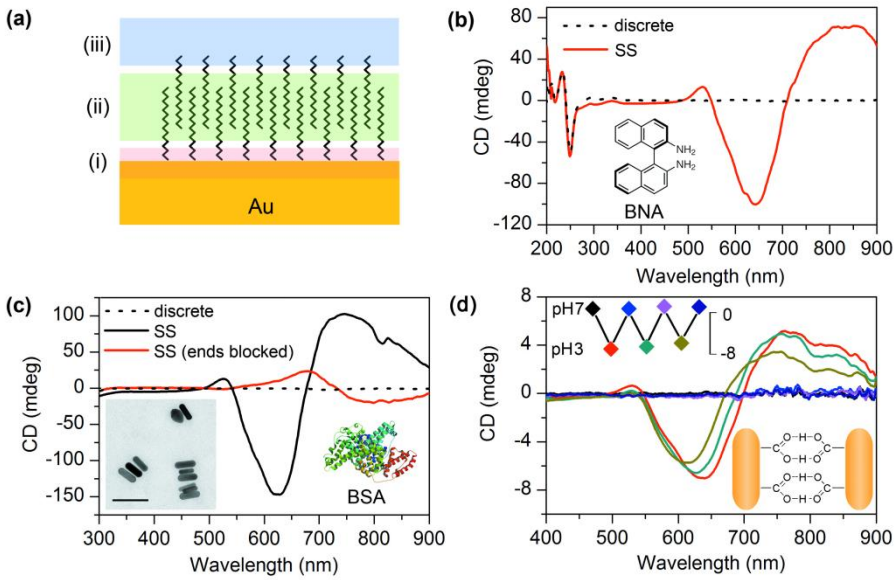

Fig. 4 Exerting twisting force from different parts of the GNRs. (a) The two interfaces and one hydrophobic region for the CATB-coated GNR: (i) the gold–surfactant interface, (ii) the hydrophobic region inside the surfactant bilayer, and (iii) the surfactant-water interface. (b) CD spectra of discrete GNRs and citrate-linked SS oligomers after enrichment of BNA in the hydrophobic bilayer. 10 μM BNA was used. (c) CD spectra of discrete GNRs, citrate-linked SS oligomers, and PEG-OMe-blocked SS oligomers after adding 5 mg/mL BSA. Inset: representative TEM image of BSA-coated oligomers (scale bar: 100 nm). (d) CD spectra of PEG-COOH-linked SS oligomers switching between pH 7 and pH 3. Inset: CD intensity at 610 nm.

on the rod. In contrast to the GNR case, where the curves for discrete nanorods and SS assemblies are drastically different, the two curves for silver-coated GNRs show similar trends, suggesting that the surface chemical anisotropy is reduced.

In principle, this reduced surface chemical anisotropy will result in smaller twist angles and hence smaller PCD signals due to the interference between L-CYS on the ends and L-CYS on the side. However, coating Ag also enhances the SPR band of the GNRs (Fig. S5, ESI†), which will increase the PCD signals. While the two factors counterbalance with each other, the former was found to play the dominate role when citrate was used as linkers. As shown in Fig. 3c, the maximum signal was only around 11 mdeg. In contrast, for the dendrimer-linked oligomers, there should be no counteraction between the twisting forces originated from the ends and the side, because L-CYS on the ends lost the twisting effect as we have discussed. Thus, the stronger SPR after Ag coating can be revealed. As shown in Fig. 3d, the maximum PCD signal (−47 mdeg) is larger than that found for GNRs without Ag coating (−33 mdeg). These results suggest that the effects of the chiral molecule location and the interparticle distance are often intertwined with each other and should be rationally designed and precisely controlled to optimize the PCD signal.

3.4 Twisting force from beyond the Au–CTAB interface

The basic idea that PCD signals can be controlled through manipulation of twisting forces can be extended to other systems. There are two interfaces and a hydrophobic region for the CTAB-coated GNR: the gold–CTAB interface, the hydrophobic region inside the CTAB bilayer, and the CTAB–water interface (illustrated in Fig. 4a).[25] In the L-CYS case, the chiral molecules are on the gold surface (or the gold–CTAB interface). Below we will show that the twisting force can also be exerted from the other parts of the GNRs when chiral molecules interact with them, and some of the phenomena observed for L-CYS, such as the location effect, are also present in these cases.

It has been established that hydrophobic molecules can be concentrated within the CTAB bilayer.[25,26] To test if chiral molecules within the CTAB bilayer can induce the twist of SS oligomers, (R)-(+)-1,1'-Binaphthyl-2,2'-diamine molecules (BNA, molecular structure shown in Fig. 4b) were added into the nanorod solution. The extinction spectrum of the GNR solution shows a red-shift immediately after the addition of BNA (Fig. S6, ESI†), suggesting the enrichment of BNA inside the CTAB bilayer. The solution of discrete GNRs modified by BNA showed CD signal only in the UV region. After linked by citrate, strong PCD emerged around the LSPR wavelength. Note that the CD signal from BNA molecules in the UV region did not change.

In Fig. 4c we show that proteins such as bovine serum albumin (BSA), which adsorb at the CTAB–water interface, are also able to induce the twist of SS oligomers. We first prepared citrate-linked SS oligomers, followed by the addition of BSA solution (extinction spectra shown in Fig. S7, ESI†). Large PCD signals (ca.150 mdeg) emerged; in comparison, discrete GNRs coated by BSA show no obvious CD around the SPR wavelength. Interestingly, the location effect was observed again: using the SS oligomers prepared from PEG-OMe modified nanorods, whose ends are inaccessible for BSA, a PCD signal of opposite sign was observed (Fig. 4c). It seems that the location effect is a general rule that applies for both the Au–CTAB interface and the CTAB–water interface. Considering the importance of protein-corona in biological applications of nanoparticles,[27] the PCD effect of protein-coated SS oligomers may serve as a novel platform to characterize the structure, composition, and conformational change of protein corona.

Finally, we replaced CTAB with HS-C_{11}-$(EG)_6$-OCH_2-COOH

(PEG-COOH) through ligand exchange (Fig. 4d), and as a result, the modified nanorods underwent spontaneous SS assembly in acidic solution, due to the formation of hydrogen bonds between the COOH groups. When the oligomer solution was incubated with L-CYS, a PCD signal emerged. The PCD signal can be manipulated by altering the pH of the solution. At pH 7, the hydrogen bond is broken (Fig. S8, ESI†) and the PCD signal vanished, showing the potential of using the system as a chiroptical switch.

4. Conclusions

We have shown that the PCD signals of SS oligomers, both the magnitude and the sign, can be manipulated through controlling the twisting force, which is highly sensitive to the chiral molecule location and the interparticle distance. Specifically, chiral molecules at the ends of the GNRs and those on the side twist the oligomers to opposite directions and induce PCD with opposite signs; the PCD signal is reduced when the interparticle distance is enlarged because of the smaller twist angle. The twisting force may be exerted from the Au–CTAB interface, the hydrophobic CTAB bilayer, or the CTAB–water interface. This system is a promising candidate for chiroptical switches and sensors (an example of sensing of enantiomeric purity is shown in Fig. S9, ESI†). These basic findings will serve as guidance for how to generate large and controllable PCD signals in future PCD-based applications. PCD could also be considered as a novel technique to study the interactions between nanoparticles. We have already seen the power of PCD in revealing subtle effects in interparticle forces, which is hardly accessible via other techniques. A deeper understanding of the twisting force will need further experiments and multiscale simulations, which should take both molecular scale and nanoscale effects into account.

Acknowledgements

The work was supported by the National Key Basic Research Program of China (2012CB934001 and 2011CB932802) and the National Natural Science Foundation of China (Grant No. 91127013 and 21173056).

Notes and references

[a] *CAS Key Laboratory of Standardization and Measurement for Nanotechnology, National Center for Nanoscience and Technology, Beijing 100190, China. E-mail: wuxc@nanoctr.cn, huzj@nanoctr.cn*
[b] *University of the Chinese Academy of Sciences, Beijing 100049, China*

† Electronic Supplementary Information (ESI) available: L-NAC and L-GSH induced PCD signal; electric field profile of a single GNR and an SS tetramer; SERS spectra of 4-MP modified discrete GNRs and SS oligomers; extinction spectra; and application in enantiomeric purity sensing. See DOI: 10.1039/b000000x/

1 V. K. Valev, J. J. Baumberg, C. Sibilia, T. Verbiest, *Adv. Mater.*2013, **25**, 2517.
2 A. Guerrero-Martínez, J. L. Alonso-Gómez, B. Auguié, M. M. Cid, L. M. Liz-Márzan, *Nano Today*2011, **6**, 381.
3 A. Ben-Moshe, B. M. Maoz, A. O. Govorov, G. Markovich, *Chem. Soc. Rev.*2013, **42**, 7028.
4 E. Hendry, T. Carpy, J. Johnston, M. Popland, R. V. Mikhaylovskiy, A. J. Lapthorn, S. M. Kelly, L. D. Barron, N. Gadegaard, M. Kadodwala, *Nat. Nanotechnol.*2010,**5**, 783.
5 Y. Zhao, L. G. Xu, W. Ma, L. B. Wang, H. Kuang, C. L. Xu, N. A. Kotov, *Nano Lett.*2014, **14**, 3908.
6 X. L. Wu, L. G. Xu, L. Q. Liu, W. Ma, H. H. Yin, H. Kuang, L. B. Wang, C. L. Xu, N. A. Kotov, *J. Am. Chem. Soc.*2013, **135**, 18629.
7 W. Ma, H. Kuang, L. G. Xu, L. Ding, C. L. Xu, L. B. Wang, N. A. Kotov, *Nat. Commun.*2013, **4**, 2689.
8 W. Chen, A. Bian, A. Agarwal, L. Q. Liu, H. B. Shen, L. B. Wang, C. L. Xu, N. A. Kotov, *Nano Lett.*2009, **9**, 2153.
9 A. Kuzyk, R. Schreiber, Z. Y. Fan, G. Pardatscher, E.-M. Roller, A. Högele, F. C. Simmel, A. O. Govorov, T. Liedl, *Nature*2012, **483**, 311.
10 S. H. Jung, J. Jeon, H. Kim, J. Jaworski, J. H. Jung, *J. Am. Chem. Soc.*2014, **136**, 6446.
11 R.-Y. Wang, H. L. Wang, X. C. Wu, Y. L. Ji, P. Wang, Y. Qu, T.-S. Chung, *Soft Matter*2011, **7**, 8370.
12 A. Guerrero-Martínez, B. Auguié, J. L. Alonso-Gómez, Z. Džolić, S.Gómez-Graña, M. Žinić, M. M. Cid, L. M. Liz-Marzán, *Angew. Chem. Int. Ed.*2011, **50**, 5499.
13 A. Querejeta-Fernández, G. Chauve, M. Methot, J. Bouchard, E.Kumacheva, *J. Am. Chem. Soc.*2014, **136**, 4788.
14 S. Hou, T. Wen, H. Zhang, W. Q. Liu, X. N. Hu, R. Y. Wang, Z. J. Hu, X. C. Wu, *Nano Res.* 2014, **7**, 1699.
15 W. Ma, H. Kuang, L. Wang, L. Xu, W.-S. Chang, H. Zhang, M. Sun, Y. Zhu, Y. Zhao, L. Liu, C. Xu, S. Link, N. A. Kotov, *Sci. Rep.*2013, **3**, 1934.
16 X. Lan, Z. Chen, G. Dai, X. X. Lu, W. H. Ni, Q. B. Wang, *J. Am. Chem. Soc.*2013, **135**, 11441.
17 X. B. Shen, P. F. Zhan, A. Kuzyk, Q. Liu, A. Asenjo-Garcia, H.Zhang, F. J. G. de Abajo, A. Govorov, B. Q. Ding, N. Liu, *Nanoscale*, 2014, **6**, 2077.
18 A. Kuzyk, R. Schreiber, H. Zhang, A. O. Govorov, T. Liedl, N. Liu, *Nat. Mater.*2014, **13**, 862.
19 B. Auguié, J. L. Alonso-Gómez, A. Guerrero-Martínez, L. M. Liz-Marzán, *J. Phys. Chem. Lett.*2011, **2**, 846.
20 Z. Zhu, W. Liu, Z. Li, B. Han, Y. Zhou, Y. Gao, Z. Tang, *ACS Nano*2012, **6**, 2326.
21 P. B. Johnson, R. W. Christy, *Phys. Rev. B*1972, **6**, 4370.
22 H. Nakashima, K. Furukawa, Y. Kashimura, K. Torimitsu, *Chem. Commun.*2007, **10**, 1080.
23 X. Kou, S. Zhang, Z. Yang, C.-K. Tsung, G. D. Stucky, L. Sun, J.Wang, C. Yan, *J. Am. Chem. Soc.*2007, **129**, 6402.
24 X. Guo, Q.Zhang, Y. Sun, Q. Zhao, J. Yang, *ACS Nano*2012, **6**, 1165.
25 C. J. Murphy, L. B. Thompson, A. M. Alkilany, P. N. Sisco, S. P.Boulos, S. T. Sivapalan, J. A. Yang, D. J. Chernak, J. Y. Huang, *J. Phys. Chem. Lett.*2010, **1**, 2867.
26 M. A. Alaaldin, R. L. Frey,J. L. Ferry, C. J. Murphy, *Langmuir*2008, **24**, 10235.
27 J. C. Y. Kah, J. Chen, A. Zubieta, K. Hamad-Schifferli, *ACS Nano*2012, **6**, 6730.